1.392 Å) and refined with individual isotropic thermal parameters for the ring C atoms. Convergence occurred at $R_1 = \sum||F_o| - |F_c||/\sum|F_o| = 0.049$ and $R_2 = (\sum w(|F_o| - |F_c|)^2/(\sum|F_o|^2)^{1/2} = 0.053$.

All 87 H atoms were located in positive electron density in a difference Fourier synthesis ($(\sin\theta)/\lambda$ maximum 0.35) with 77 of them appearing as distinct peaks with densities varying from 0.3 (1) to 0.6 (1) e Å^{-3}. All but the hydride atom were included in idealized positions (sp^2, C–H = 0.90 Å; sp^3, C–H = 0.95 Å) with thermal parameters set at 110% of that of the atom to which they are bonded. Their positions were updated as the refinement progressed, but they were not refined. There was evidence for secondary extinction, and a correction was included.[35] Following our preliminary report,[17] a successful attempt was made to refine the hydride atom positional parameters. The final cycles of refinement included 303 variables, 8258 unique observations, and a p value of 0.04 and converged at agreement factors of $R_1 = 0.0429$ and $R_2 = 0.0420$ and a goodness-of-fit value of 2.50e. The largest parameter shift in the final cycle was 0.21σ, associated with the y coordinate of the hydride atom. The highest residual electron density was 0.9 (1) e Å^{-3} at (0.107, 0.046, –0.070), near C(23) and C(24) and was of no chemical significance. A statistical analysis on $|F_o|$, $\lambda^{-1}\sin\theta$, and various combinations of Miller indices and diffractometer setting angles showed no unusual trends and indicated a satisfactory weighting scheme.

Atomic positional and U_{eq} or U thermal parameters are listed in Table V. Additional crystallographic data are included as supplementary material.[36]

Acknowledgment. We thank the NSERC (Canada) for financial support (N.C.P., R.J.P.) and for a graduate fellowship (M.C.J.).

Registry No. **1**, 99642-80-5; **2**, 89189-82-2; **3**, 107206-14-4; **3b**, 107207-51-2; **4**, 110433-38-0; **5**, 110433-44-8; **6**, 110433-42-6; **7**, 110433-40-4; S, 7704-34-9; Se, 7782-49-2; chloroform, 67-66-3.

Supplementary Material Available: Tables SI–SV, listing derived hydrogen atom parameters, rigid-group parameters, anisotropic thermal parameters, angles and distances associated with the phenyl rings, and a weighted least-squares plane and selected torsion angles (8 pages); a table of observed and calculated structure amplitudes (37 pages). Ordering information is given on any current masthead page.

(34) Eisenberg, R.; Ibers, J. A. *Inorg. Chem.* **1965**, *4*, 773.
(35) Zachariasen, W. H. *Acta Crystallogr., Sect. A: Cryst. Phys., Diffr. Theor. Gen. Crystallogr.* **1968**, *A24*, 212–216.
(36) See paragraph describing supplementary material at the end of the paper.

Contribution from the Department of Chemistry
and Molecular Structure Center, Indiana University, Bloomington, Indiana 47405

1,2-Bis(di-*tert*-butylarsenido)tetrakis(dimethylamido)dimolybdenum and -ditungsten. Synthesis, Structures, and Solution Behavior

M. H. Chisholm,* J. C. Huffman, and J. W. Pasterczyk

Received May 27, 1987

The compounds 1,2-M_2(As-*t*-$Bu_2)_2(NMe_2)_4$ (M = Mo, W) are obtained as hydrocarbon-soluble crystalline solids in the reaction between 1,2-$M_2Cl_2(NMe_2)_4$ and 2 equiv of LiAs-*t*-Bu_2 in THF at –78 °C. Both are light-sensitive in solution; the molybdenum compound sublimes at 95 °C (10^{-4} Torr). X-ray crystal structure determinations revealed that both compounds crystallize in the anti rotameric form of the familiar 1,2-disubstituted ethane-like configuration for $X_2YM{\equiv}MX_2Y$. The metal–metal distances (2.2159 (12) Å for M = Mo, 2.3001 (11) Å for M = W) are typical for unbridged d^3–d^3 dimers. The geometries about the arsenic atoms are distinctly pyramidal, and those about the nitrogen atoms are planar, with the average M–N distances (1.972 (6) Å for M = Mo, 1.955 (9) Å for M = W) being statistically identical with those found in the corresponding $M_2(NMe_2)_6$ compounds. The Mo–As and W–As distances (2.6163 (11) and 2.5949 (15) Å, respectively) are the first measured M–As distances for a transition-metal compound with a terminal arsenido ligand. The solution behavior of these compounds, as investigated by variable-temperature ^{1}H NMR spectroscopy, corresponds to 1:1 mixtures of anti and gauche rotamers interconverting slowly on the NMR time scale. Interpretation of these spectra requires rotation about the M–N and M–As bonds, the latter process having a lower energy barrier than the former, as well as rapid inversion of the arsenic atoms. These results indicate considerably more ground-state π-bond character between the metal and nitrogen atoms than between the metal and arsenic atoms. Crystal data for Mo_2(As-*t*-$Bu_2)_2(NMe_2)_4$ at –155 °C: $a = 14.841$ (3) Å, $b = 10.478$ (2) Å, $c = 10.367$ (1) Å, $\beta = 90.84$ (1)°, $Z = 2$, $d_{calcd} = 1.538$ g cm^{-3}, monoclinic space group $P2_1/n$. Crystal data for W_2(As-*t*-$Bu_2)_2(NMe_2)_4$ at –153 °C: $a = 14.795$ (5) Å, $b = 10.505$ (3) Å, $c = 10.379$ (3) Å, $\beta = 91.14$ (2)°, $Z = 2$, $d_{calcd} = 1.899$ g cm^{-3}, monoclinic space group $P2_1/n$.

Introduction

The coordination chemistry of the $(Mo{\equiv}Mo)^{6+}$ and $(W{\equiv}W)^{6+}$ units has been the subject of intensive investigation for more than a decade and has continued to yield fascinating results.[1] However, the bulk of this work has been performed for ligands coordinated to the metals by second-row main-group atoms, specifically carbon, nitrogen, and oxygen. Sufficient chemical differences exist between the second-row elements and their heavier congeners,[2] however, to warrant a more thorough investigation of the use of heavy main-group anionic ligands in dinuclear transition-metal chemistry.

Efforts in our laboratories in this vein have heretofore been limited primarily to thiolate[3] and phosphido[4] ligands. A number of reasons make arsenic, in addition, an attractive element to incorporate into an organometallic compound. Weaker metal–arsenic and carbon–arsenic bonds[5] compared to those of its lighter congeners raise the possibility of facile thermolysis or photolysis of compounds whose molecular structures are well-known, possibly affording higher nuclearity clusters via mechanistically interesting routes, or perhaps yielding solid-state materials with unique and useful photochemical, magnetic, or electrical properties. This latter prospect is particularly intriguing considering the current interest

(1) (a) Chisholm, M. H. *Polyhedron* **1983**, *2*, 681. (b) Chisholm, M. H.; Cotton, F. A. *Acc. Chem. Res.* **1978**, *11*, 356. (c) Chisholm, M. H. *Transition Met. Chem.* **1978**, *3*, 321. (d) Chisholm, M. H. *Angew. Chem., Int. Ed. Eng.* **1986**, *25*, 21.
(2) See, e.g.: Greenwood, N. N.; Earnshaw, A. *Chemistry of the Elements*; Pergamon: Oxford, 1984.
(3) Chisholm, M. H.; Corning, J. F.; Folting, K.; Huffman, J. C. *Polyhedron* **1985**, *4*, 383 and references therein.
(4) Buhro, W. E.; Chisholm, M. H.; Folting, K.; Huffman, J. C. *J. Am. Chem. Soc.* **1987**, *109*, 905
(5) Dasent, W. E. *Inorganic Energetics*; Penquin: Harmondsworth, England, 1970.

0020-1669/87/1326-3781$01.50/0

Table I. Summary of Crystal Data

mol formula	$Mo_2As_2N_4C_{24}H_{60}$	$W_2As_2N_4C_{24}H_{60}$
color of cryst	dark red	orange at 25 °C yellow at −153 °C
cryst dimens, mm	0.23 × 0.23 × 0.33	0.032 × 0.040 × 0.060
space group	$P2_1/n$	$P2_1/n$
temp, °C	−155	−153
cell dimens		
a, Å	14.841 (3)	14.795 (5)
b, Å	10.478 (2)	10.505 (3)
c, Å	10.367 (1)	10.379 (3)
β, deg	90.84 (1)	91.14 (2)
Z (molecules/cell)	2	2
vol, Å^3	1611.92	1612.86
calcd density, s/cm^3	1.538	1.899
wavelength, Å	0.71069	0.71069
mol wt	746.49	922.31
linear absd coeff, cm^{-1}	28.112	93.315
scan method	θ–2θ	θ–2θ
detector–sample dist, cm	22.5	22.5
sample–source dist, cm	23.5	23.5
av ω scan width at half-height, deg	0.25	0.25
scan speed, deg/min	4.0	4.0
scan width, deg + dispersion	2.0	1.8
individual bkgd, s	8	8
aperture size, mm	3.0 × 4.0	3.0 × 4.0
2θ range, deg	6–45	6–55
tot. no. of reflcns collcd	3558	7007
no. of unique intensities	2085	2858
no. with $F > 3\sigma(F)$	1743	2236
$R(F)$	0.0395	0.0429
$R_w(F)$	0.0396	0.0373
goodness of fit for the last cycle	0.942	0.891
max Δ/σ for last cycle	0.05	0.5

Table II. Fractional Coordinates and Isotropic Thermal Parameters for $Mo_2(As\text{-}t\text{-}Bu_2)_2(NMe_2)_4$

atom	10^4x	10^4y	10^4z	$10B_{iso}$, Å^2
Mo(1)	458.0 (4)	9363 (1)	4464 (1)	10
N(2)	59 (4)	7630 (5)	4953 (6)	12
C(3)	480 (7)	6575 (8)	4275 (9)	21
C(4)	−616 (6)	7172 (8)	5802 (9)	19
N(5)	315 (4)	9898 (6)	2656 (6)	13
C(6)	709 (6)	9058 (9)	1678 (8)	20
C(7)	−225 (6)	10883 (8)	2006 (8)	18
As(8)	2029 (1)	9613 (1)	5614 (1)	15
C(9)	2956 (5)	9178 (7)	4255 (7)	17
C(10)	3919 (6)	9204 (9)	4826 (10)	24
C(11)	2762 (7)	7806 (8)	3855 (10)	25
C(12)	2911 (7)	10049 (9)	3074 (9)	24
C(13)	2474 (5)	11228 (7)	6508 (7)	18
C(14)	3177 (7)	10833 (10)	7520 (9)	27
C(15)	1678 (6)	11835 (8)	7215 (9)	21
C(16)	2887 (7)	12236 (9)	5601 (10)	24

in gallium arsenide as a semiconductor.[6] Our first efforts in this direction are presented herein.

Results and Discussion

Synthesis and Physicochemical Properties. $1,2\text{-}M_2(As\text{-}t\text{-}Bu_2)_2(NMe_2)_4$ (M = Mo (**1**), W (**2**)) compounds are prepared in high yield by the simple arsenide-for-halide exchange reaction depicted in eq 1. Similar reactions have been used to prepare

$$1,2\text{-}M_2Cl_2(NMe_2)_4 + 2LiAs\text{-}t\text{-}Bu_2 \xrightarrow[-78\ °C]{THF} 1,2\text{-}M_2(As\text{-}t\text{-}Bu_2)_2(NMe_2)_4 + 2LiCl \quad (1)$$

M = Mo, W

the analogous bis(phosphide)[4] and bis(alkyl)[7] compounds as well as a host of other mono-[8] and dinuclear[9] arsenido complexes. Both of the new compounds are air- and water-sensitive, although the tungsten compound is much less so, and both are light-sensitive

Table III. Fractional Coordinates and Isotropic Thermal Parameters for $W_2(As\text{-}t\text{-}Bu_2)_2(NMe_2)_4$

atom	10^4x	10^4y	10^4z	$10B_{iso}$, Å^2
W(1)	471.3 (3)	9336.4 (4)	4442.9 (4)	10
N(2)	74 (6)	7629 (9)	4931 (10)	14
C(3)	458 (10)	6524 (13)	4265 (15)	21
C(4)	−607 (9)	7157 (12)	5822 (14)	18
N(5)	328 (6)	9868 (9)	2649 (9)	11
C(6)	703 (10)	9017 (16)	1658 (12)	24
C(7)	−208 (9)	10872 (12)	2006 (12)	19
As(8)	2032 (1)	9586 (1)	5602 (1)	13
C(9)	2968 (8)	9137 (13)	4263 (11)	17
C(10)	3917 (8)	9165 (13)	4859 (13)	20
C(11)	2764 (8)	7768 (14)	3840 (15)	23
C(12)	2931 (9)	10026 (14)	3070 (13)	23
C(13)	2481 (8)	11211 (12)	6475 (12)	18
C(14)	3204 (9)	10815 (16)	7506 (13)	23
C(15)	1707 (9)	11811 (14)	7181 (14)	21
C(16)	2909 (10)	12187 (14)	5597 (16)	24

Table IV. Pertinent Structural Parameters for $1,2\text{-}M_2(As\text{-}t\text{-}Bu_2)_2(NMe_2)_4$[a]

parameter	M = Mo	M = W
M–M	2.2159 (12)	2.3001 (11)
M–As	2.6163 (11)	2.5949 (15)
M–N (av)	1.972 (6)	1.955 (9)
As–C (av)	2.035 (7)	2.038 (11)
N–C (av)	1.453 (10)	1.473 (15)
M′–M–As	105.10 (4)	104.38 (4)
M′–M–N (av)	104.00 (17)	104.12 (28)
M–N–C (av)	133.4 (5),[b] 116.3 (5)[c]	133.3 (8),[b] 117.9 (8)[c]
As–M–N	119.30 (18),[d] 104.09 (17)[e]	119.47 (26),[d] 104.0 (3)[e]
N–M–N	118.54 (24)	118.8 (4)
M–As–C	124.87 (22),[b] 105.62 (22)[c]	124.8 (4),[b] 105.7 (4)[c]
C–As–C	106.5 (3)	106.1 (5)
C–N–C (av)	110.0 (6)	108.4 (10)

[a] Distances in angstroms; angles in degrees. [b] Proximal to the M–M bond. [c] Distal to the M–M bond. [d] Adjacent to *tert*-butyl groups. [e] Adjacent to arsenic lone pair.

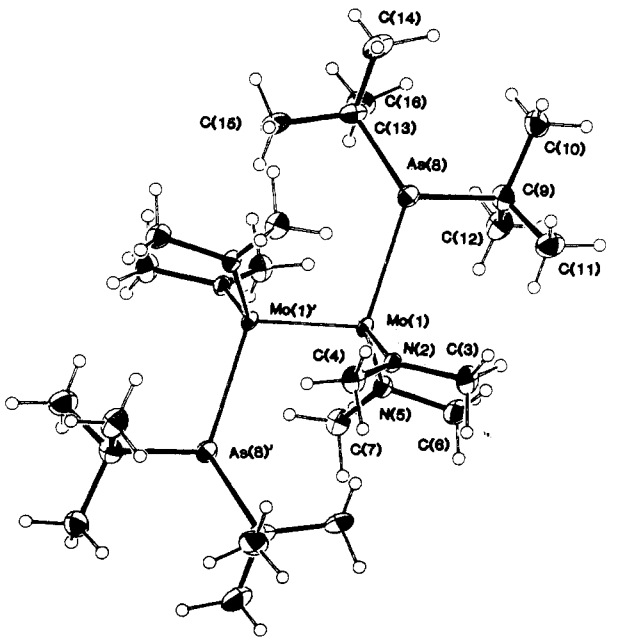

Figure 1. ORTEP diagram of $1,2\text{-}Mo_2(As\text{-}t\text{-}Bu_2)_2(NMe_2)_4$. Atomic positions are represented by 50% probability thermal ellipsoids.

(6) Keyes, R. W. *Science (Washington, DC)* **1985**, *230*, 138.
(7) Chisholm, M. H.; Haitko, D. A.; Folting, K.; Huffman, J. C. *J. Am. Chem. Soc.* **1981**, *103*, 4046.
(8) (a) Pitt, C. G.; Higa; K. T.; McPhail, A. T.; Wells, R. L. *Inorg. Chem.* **1986**, *25*, 2483. (b) Malisch, W.; Luksza, M.; Sheldrick, W. S. *Z. Naturforsch., B: Anorg. Chem., Org. Chem.* **1981**, *36B*, 1580. (c) Wade, S. R.; Wallbridge, M. G. H.; Willey, G. R. *J. Organomet. Chem.* **1984**, *267*, 271.

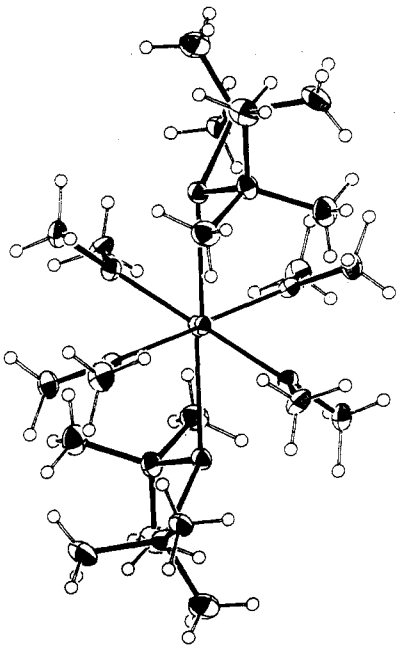

Figure 2. ORTEP diagram of 1,2-Mo_2(As-*t*-Bu_2)$_2$(NMe_2)$_4$ viewed down the metal–metal axis, showing planarity at the nitrogen atoms and pyramidality at the arsenic atoms. Atomic positions are represented by 50% probability thermal ellipsoids.

in solution but light-stable in the solid state. They are soluble in hexane, toluene, benzene, and THF, and the molybdenum compound sublimes at 95 °C (10^{-4} Torr) with minor decomposition of the residue, while the tungsten analogue slowly decomposes at 85 °C under a dynamic vacuum. The molybdenum compound crystallizes as analytically pure dark red plates from hexane; the tungsten compound, as orange cubes from toluene.

Solid-State and Molecular Structures. Crystal data for **1** and **2** are summarized in Table I. Fractional coordinates and isotropic thermal parameters for **1** and **2** are given in Table II and III, respectively. Pertinent bond distances and angles are summarized in Table IV. ORTEP diagrams of **1** are given in Figures 1 and 2.

Both compounds crystallize in the anti conformation of the 1,2-disubstituted ethane-like geometry and are isostructural. Their metal–metal distances are representative for molybdenum and tungsten d^3–d^3 dimers[1] and are essentially identical with those of their respective hexakis(amido) parent compounds.[10] The Mo–Mo distance is within 3σ of that found in the *anti*-bis(phosphido) analogue,[4] and the W–W distance is only slightly shorter than those found in both the anti and gauche rotamers of 1,2-W_2(P-*t*-Bu_2)$_2$(NMe_2)$_4$.[4,11] The M–N distances and M′–M–N angles are also representative for this class of compounds.[4,7,10,11]

1 and **2** contain planar nitrogen atoms, which, together with the short M–N distances, are indicative of a large degree of M–N π-bond character. This is also reflected in the difference between the M–N–C angles that are proximal and distal to the M≡M bonds. Steric repulsions between the proximal *N*-methyl groups of one metal atom and the *tert*-butyl groups of the other metal atom force the ligands apart, opening up the proximal M–N–C angles rather than twisting the dimethylamido ligands about the M–N axis, which would decrease across-bond steric repulsion but sacrifice N_p–M_d π overlap and thus decrease M–N π-bond stabilization. This steric crowding also opens up the proximal M–As–C angles compared to the respective distal angles. The larger steric bulk of the *tert*-butyl groups versus that of the arsenic lone pairs is responsible for enlarging the As–M–N angles adjacent to the *tert*-butyl groups.

Table V. Barriers to Rotation, ΔG^*_T (T_c) (kcal/(mol K)), about M–N Bonds in 1,2-M_2(As-*t*-Bu_2)$_2$(NMe_2)$_4$ Compounds

bond	M = Mo	M = W
gauche M–N	12.0 ± 0.8 (273)	11.1 ± 0.8 (253)
gauche M–N′	11.6 ± 0.8 (258)	10.5 ± 0.9 (233)
anti M–N	8.1 ± 0.9 (188)	*a* (189)

[a] Poor solubility below 189 K prevented observation of the proximal and distal *N*-methyl signals.

The arsenic atoms of both compounds display a trigonal-pyramidal coordination geometry (Figure 2), the sums of angles about arsenic being 337.0 and 336.6° for **1** and **2**, respectively. These indicate a large amount of p character in the bonding orbitals of arsenic and a proportionally large amount of s character in the arsenic lone pairs, reflecting the well-known propensity for heavier main-group atoms to minimize hybridization[12] (the inert s-pair effect). Similarly small sums of angles about arsenic are found in [(mesityl)$_2$As]$_3$Ga,[8a] arsine, and the arsenic trihalides.[14]

To the best of our knowledge, these compounds represent the first structurally characterized examples of arsenido ligands terminally coordinated to transition-metal centers,[13] so direct comparisons of M–As distances are not possible. It can be pointed out, however, that the sums of the M_2^{6+} (M = Mo, W) covalent radii (1.40 Å)[1a] and the Pauling covalent or tetrahedral covalent arsenic radii (1.21 and 1.18 Å, respectively)[15] are reasonably close to the observed M–As distances. The Mo–As distance is only slightly longer than the average of those found in [Cp-$(CO)_2$Mo(μ-AsMe_2)]$_2$ of 2.607 Å[16] and similar to those found in a series of cyclopolyarsanes bound to molybdenum carbonyl units,[17] although the arsenic moieties of the latter are only dative-bound to the metal centers. Both the pyramidality of arsenic and the long M–As distances argue against any M–As π-bonding effects in **1** or **2**. This parallels the bonding mode of phosphorus in the anti rotamers of the bis(phosphido) analogues.[4,11]

Solution Behavior of 1,2-M_2(As-*t*-Bu_2)$_2$(NMe_2)$_4$ (M = Mo, W). A crystalline sample of the anti rotamer of Mo_2(As-*t*-Bu_2)$_2$-(NMe_2)$_4$ dissolved at room temperature displays variable-temperature ^{1}H NMR spectra too complicated to explain solely on the basis of the solid-state structure (Figure 3). At 80 °C the spectrum displays two *tert*-butyl signals in an approximately 1:1 ratio and three *N*-methyl signals in an approximately 1:2:1 ratio. As the sample is cooled to −10 °C, the two lesser intensity *N*-methyl signals collapse into the base line. At −20 °C the remaining *N*-methyl signal begins to broaden and a pair of signals appears whose average chemical shift equals that of the most downfield 80 °C *N*-methyl signal. The most upfield *N*-methyl signal at 80 °C likewise reappears as a pair of signals at −30 °C. These four signals continue to sharpen at lower temperatures. The third 80

(9) (a) Hieber, W.; Kummer, R. *Chem. Ber.* **1967**, *100*, 148. (b) Jones, R. A.; Whittlesey, B. R. *J. Am. Chem. Soc.* **1985**, *107*, 1078. (c) Jones, R. A.; Whittlesey, B. R. *Organometallics* **1984**, *3*, 469. (d) Jones, R. A.; Whittlesey, B. R. *Inorg. Chem.* **1986**, *25*, 852. (e) Arif, A. M.; Jones, R. A.; Seeberger, M. H.; Whittlesey, B. R.; Wright, T. C. *Inorg. Chem.* **1986**, *25*, 3943.

(10) (a) Chisholm, M. H.; Cotton, F. A.; Frenz, B. A.; Reichert, W. W.; Shive, L. W.; Stults, B. R. *J. Am. Chem. Soc.* **1976**, *98*, 4469. (b) Chisholm, M. H.; Cotton, F. A.; Extine, M.; Stults, B. R. *J. Am. Chem. Soc.* **1976**, *98*, 4477.

(11) The structure of *anti*-1,2-W_2(P-*t*-Bu_2)$_2$(NMe_2)$_4$ has been determined. Pertinent structural parameters that differ significantly from those found in the gauche rotamer: W–W, 2.3091 (5) Å; W–P, 2.4695 (15) Å; W–W–P, 105.27 (4)°; W–P–C_{prox}, 129.95 (17)°; W–P–C_{dist}, 108.24 (18)°. Buhro, W. E.; Chisholm, M. H.; Huffman, J. C.; Streib, W. E., unpublished results.

(12) Kutzelnigg, W. *Angew. Chem., Int. Ed. Engl.* **1984**, *23*, 272.

(13) (a) The structure of [(mesityl)$_2$As]$_3$Ga has recently been reported,[8a] as well as that for the terminal arsaalkyne compound (η^5-C_5H_5)-$(CO)_2$Fe—As≡C(OSiMe_3)(*t*-Bu).[8b] (b) Weber, L.; Meine, G.; Boese, R. *Angew. Chem., Int. Ed. Engl.* **1986**, *25*, 469.

(14) (a) Harmony, M. D.; Laurie, V. W.; Kuczkowski, R. L.; Schwendeman, R. H.; Ramsey, I. A.; Lovas, F. J.; Lafferty, W. J.; Maki, A. G. *J. Phys. Chem. Ref. Data* **1979**, *8*, 619. (b) Konaka, S.; Kimura, M. *Bull. Chem. Soc. Jpn.* **1970**, *43*, 1693.

(15) Pauling, L. *The Nature of the Chemical Bond*, 2nd ed.; Cornell University Press: Ithaca, NY, 1948.

(16) Gross, E.; Burschka, C.; Malisch, W. *Chem. Ber.* **1986**, *119*, 378.

(17) (a) Rheingold, A. L.; Fountain, M. E. *Organometallics* **1986**, *5*, 2410. (b) Rheingold, A. L.; Fountain, M. E.; DiMaio, A. J. *J. Am. Chem. Soc.* **1987**, *109*, 141.

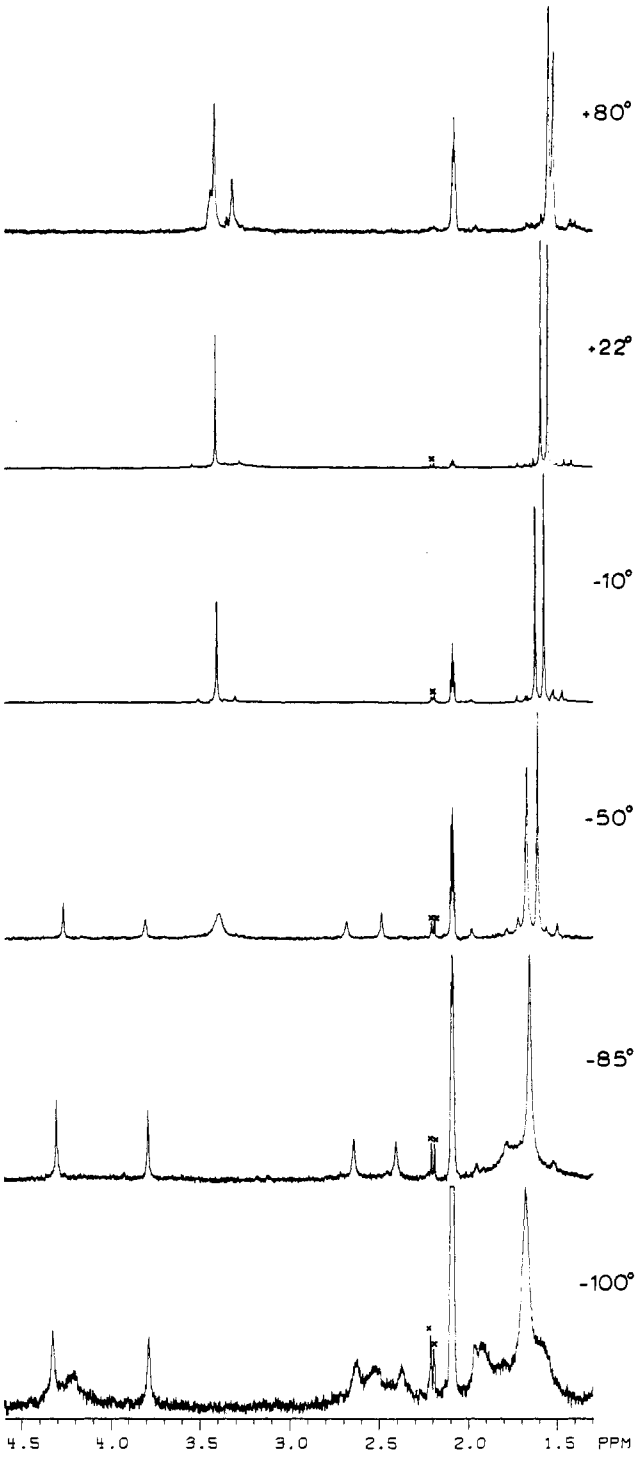

Figure 3. Variable-temperature ^1H NMR spectra of 1,2-Mo_2(As-*t*-Bu_2)$_2$(NMe_2)$_4$ in toluene-d_8. Peaks labeled by an × are due to impurities.

°C *N*-methyl signal collapses into the base line at −85 °C and reappears at −100 °C as a pair of signals. The downfield *tert*-butyl resonance coalesces at ca. −90 °C and also reappears as two signals at −100 °C. The remaining *tert*-butyl resonance begins to broaden at −85 °C but fails to coalesce into the base line by −100 °C.

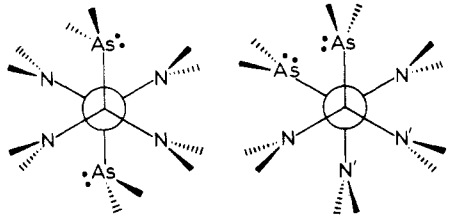

Table VI. Barriers to Rotation about M–N Bonds in M_2^{6+} Amido Compounds

compd	$\Delta G^{\ddagger}$, kcal mol^{-1}	T_c, °C	ref
$Mo_2(NMe_2)_6$	11.5 ± 0.2	−30 ± 2	10a
$Mo_2(NEt_2)_6$	13.6 ± 0.5	16 ± 5	10a
$W_2(NMe_2)_6$	11.2 ± 0.2	−35 ± 2	10b
$W_2(NEt_2)_6$	13.3 ± 0.4	10 ± 5	10b
anti-1,2-$Mo_2Cl_2(NMe_2)_4$	14.1		23
anti-1,2-$W_2Cl_2(NMe_2)_4$	13.9		23
anti-1,2-Mo_2(P-*t*-Bu_2)$_2$(NMe_2)$_4$	7.1 ± 0.2	−108	4
gauche-1,2-Mo_2(P-*t*-Bu_2)$_2$(NMe_2)$_4$	11.5 ± 0.1	−13	4
	8.2 ± 0.1	−88	
anti-1,2-W_2(P-*t*-Bu_2)$_2$(NMe_2)$_4$	7.3 ± 0.2	−103	4
gauche-1,2-W_2(P-*t*-Bu_2)$_2$(NMe_2)$_4$	11.3 ± 0.1	−17	4
	7.5 ± 0.1	−103	

These data are consistent with a 1:1 mixture of anti and gauche rotamers that are interconverting slowly on the NMR time scale. A procedure consisting of dissolving a crystalline sample of the known anti rotamer at −78 °C and recording its ^1H NMR spectrum at −50 °C without allowing it to warm to room temperature and then warming it to 20 °C and rerecording its spectrum at −50 °C confirms that the greatest intensity *N*-methyl signal and the upfield *tert*-butyl resonance seen at +80 °C correspond to the anti rotamer, the other signals thus belonging to the gauche rotamer. Activation barriers[18] and coalescence temperatures for M–N bond rotations are presented in Table V. Comparisons with several other M_2^{6+} amido compounds are provided in Table VI. The magnetic anisotropy of the metal-metal triple bond accounts for the large chemical shift difference between the proximal and distal *N*-methyl resonances below the coalescence temperature and is analogous to the behavior of the parent dinuclear hexaamides.[10a]

At ca. −90 °C the single *tert*-butyl resonance for the gauche rotamer coalesces into the base line with an energy of activation of $\Delta G^{\ddagger} = 8.5 \pm 0.9$ kcal mol^{-1}, reappearing at −100 °C as a pair of signals. Above the coalescence temperature the mechanism for equivalencing the *tert*-butyl groups must involve both rapid rotation about the Mo–As bond and a time-averaged planar geometry about arsenic, implying rapid inversion of the arsenic atom, most likely via a transition state involving some degree of stabilization via $As_p \rightarrow Mo_d$ dative π bonding permitted by the electronic unsaturation of the Mo_2^{6+} core. Although rotation about a Mo–As partial double bond would be expected to be hindered, the low measured barriers to rotation about the formal M≒As bonds in $Cp(CO)_2M(\doteqdot As\text{-}t\text{-}Bu_2)$ of 10.9 and 11.1 kcal mol^{-1} for M = Mo and W, respectively,[19] suggest that the barrier in *gauche*-**1** may be similarly low, as does the rapid Mo–As bond rotation at −100 °C in *anti*-**1**.

Below the coalescence temperature there are three basic mechanisms that can explain the two-signal pattern for the gauche *t*-Bu resonances: (a) rapid rotation about the Mo–As bond with slowed inversion at arsenic; (b) rapid inversion at arsenic but frozen-out Mo–As bond rotation; (c) frozen-out rotation and inversion. It is unlikely that both processes, shown in (c), would become slow on the NMR time scale at the same temperature, and scenario (a) would be expected to give two signals with a very small difference in chemical shifts since (a) pairwise equivalences a proximal *tert*-butyl group with a distal *tert*-butyl group and vice versa, so (b) is considered the most likely possibility. Again, some degree of $As_p \rightarrow Mo_d$ dative π bonding in the transition state is postulated to be responsible for the facile inversion at the As atom, particularly since inversion of AsH_3 through a D_{3h} transition state has been calculated to have a barrier of $\Delta E_0 = 40.6$ kcal mol^{-1}.[20] A similar mechanism has been invoked to explain rapid inversion about the phosphide phosphorus atom of $CpRe(NO)(PPh_3)$(P-

(18) Sandstrom, J. *Dynamic NMR Spectroscopy*; Academic: New York, 1982; pp 79, 109.
(19) Luksza, M.; Himmel, S.; Malisch, W. *Angew. Chem., Int. Ed. Engl.* **1983**, *22*, 416.
(20) Dixon, D. A.; Arduengo, A. J., III. *J. Am. Chem. Soc.* **1987**, *109*, 338.

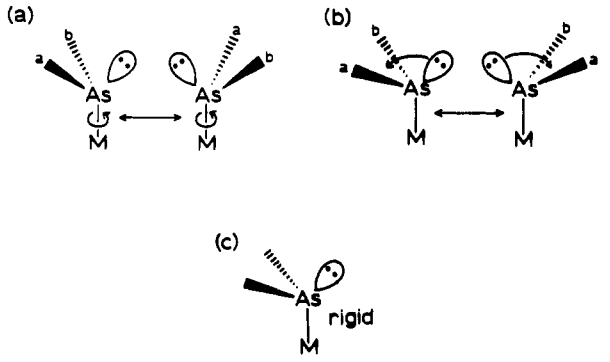

(*p*-tolyl)$_2$).[21] A moderate amount of P→W π bonding is in fact observed in the solid-state structure of *gauche*-1,2-W_2(P-*t*-Bu_2)$_2$(NMe_2)$_4$ compared to the case of its anti rotamer, which displays little if any.[4,11] These data serve as examples of the observation that π bonding to the $(M{\equiv}M)^{6+}$ moiety involving heavier main-group elements is generally weak compared to that involving second-row atoms.[22]

The tungsten compound **2** displays variable-temperature ^{1}H NMR behavior qualitatively similar to that of the molybdenum compound **1**. However, only the activation barriers to rotation about the gauche rotamer's W–N bonds could be measured due to the compound's low solubility below −85 °C. The gauche rotamer's *tert*-butyl signals coalesce at T_c = −100 °C, but again low solubility prevented measuring ΔG^* for this process.

Experimental Section

All reactions were performed under dry N_2 atmospheres by using standard Schlenk techniques. Solvents were dried and deoxygenated by standard methods. ^{1}H NMR spectra were recorded at 360 MHz and are referenced to $C_6D_5CD_2H$ δ = 2.09 ppm. Infrared spectra were obtained as Nujol mulls between CsI plates. The new compounds gave satisfactory elemental analyses. They are appreciably photosensitive in solution as well as toxic, so work was performed in a fume hood under subdued lighting with the use of aluminum-foil-wrapped glassware. M_2Cl_2(NMe_2)$_4$ (M = Mo, W) compounds[23] and LiAs-*t*-Bu_2[24] were prepared according to literature procedures.

Preparation of Mo_2(As-*t*-Bu_2)$_2$(NMe_2)$_4$. A 50-mL round-bottom Schlenk flask equipped with a stirbar was charged with Mo_2Cl_2(NMe_2)$_4$ (350 mg, 0.797 mmol), 10 mL of THF was added via syringe, and the resulting yellow-green suspension was cooled to −78 °C. LiAs-*t*-Bu_2·$^1/_2Et_2O$ (372 mg, 1.595 mmol) was added in portions with stirring over 25 min, the suspension turning deep red. The suspension was stirred an additional 20 min; then the cold bath was removed and the solvent removed in vacuo. The product was extracted from LiCl with 20 mL of hexane. Cooling the extract to −20 °C produced crystals of Mo_2(As-*t*-Bu_2)$_2$(NMe_2)$_4$ as dark red plates suitable for X-ray diffraction analysis. Yield: 100 mg, 17% crystalline yield based on Mo. The yield by ^{1}H NMR is nearly quantitative. IR data (cm^{-1}): 2815 vs, 2772 vs, 1418 s, 1411 s, 1358 s sh, 1354 s, 1350 s, 1239 s sh, 1235 vs, 1157 vs, 1148 vs sh, 1137 vs, 1121 s, 1041 s, 1036 s, 1020 s, 1017 m sh, 952 vs, 939 vs, 562 s br, 354 m br, 217 m sh, 200 s tailing into the far-IR region. The compound sublimes intact under dynamic vacuum (95 °C, 10^{-4} Torr) onto a water-cooled probe, although the residue suffers a small amount of decomposition.

Preparation of W_2(As-*t*-Bu_2)$_2$(NMe_2)$_4$. The procedure is identical with that for the molybdenum analogue. X-ray-quality crystals were obtained as orange cubes by cooling a saturated toluene solution to −20 °C. ^{1}H NMR data (23 °C): δ = 1.58 (s, anti-*t*-*Bu*), 1.61 (s, gauche-*t*-*Bu*), 3.27 (s, br, gauche-N*Me*$_2$), 3.39 (s, anti-N*Me*$_2$). IR data (cm^{-1}): 2820 vs, 2773 vs, 1418 m, 1414 m, 1356 s, 1353 s, 1351 s, 1245 s sh, 1240 s, 1158 vs, 1148 s sh, 1137 s, 1127 s, 1040 s, 1036 s, 1020 s, 954 vs, 939 vs, 560 s br, 360 s br, 220 m sh, 208 s tailing into the far-IR region. The compound does not sublime but rather decomposes at 85 °C under a dynamic vacuum.

Crystallographic Studies. General procedures and listings of programs have been reported.[25] Crystal data are summarized in Table I.

Mo_2(As-*t*-Bu_2)$_2$(NMe_2)$_4$. A suitable crystal was located and transferred to the goniostat by using standard inert-atmosphere handling techniques; it was then cooled to −155 °C for characterization and data collection. A systematic search of a limited hemisphere of reciprocal space located a set of diffraction maxima with symmetry and systematic absences corresponding to the unique monoclinic space group $P2_1/n$. Subsequent solution and refinement of the structure confirmed this choice.

Data were collected in the usual manner using a continuous θ–2θ scan with fixed backgrounds. Data were reduced to a unique set of intensities and associated σ's in the usual manner. The structure was solved by a combination of direct-methods (MULTAN78) and Fourier techniques. The positions of all hydrogen atoms were clearly visible in a difference Fourier phased on the non-hydrogen atoms, and the coordinates and isotropic thermal parameters for hydrogens were varied in the final cycles of refinement. The molecule has a crystallographic center of symmetry. A ψ scan of several reflections near χ = 90 ° indicated that no absorption correction was necessary. A final difference Fourier was essentially featureless, with the largest peak being 1.3 e/Å^3 located adjacent to the metal position.

W_2(As-*t*-Bu_2)$_2$(NMe_2)$_4$. A suitable small crystal was selected and transferred to the goniostat, where it was cooled to −153 °C for characterization and data collection. A systematic search of a limited hemisphere of reciprocal space yielded a set of reflections that exhibited monoclinic symmetry and systematic extinctions of $h0l$ for $h + l = 2n + 1$ and of $0k0$ for $k = 2n + 1$. The choice of the space group $P2_1/n$ was confirmed by the solution and refinement of the structure.

Data were collected in the usual manner to a maximum 2θ = 55°. An absorption correction was carried out, the R value for the averaging of equivalent reflections being 0.068 before the correction and 0.056 after. The R value for the averaging was computed for 2353 reflections observed more than once.

The structure was solved by the use of direct methods and Fourier techniques. The non-hydrogen atoms were readily located, and almost all of the hydrogen atoms were visible in a subsequent difference Fourier. The full-matrix least-squares refinement was completed by using anisotopic thermal parameters on all non-hydrogen atoms and isotropic thermal parameters on the hydrogen atoms. The molecular structure has a crystallographic center of symmetry. The final difference Fourier was essentially featureless, the largest peak being 1.6 e/Å^3 adjacent to the tungsten position.

Acknowledgment. We thank the National Science Foundation and the Wrubel Computing Center for support.

Registry No. **1**, 110486-14-1; **2**, 110486-15-2; $Mo_2Cl_2(NMe_2)_4$, 63301-82-6; $W_2Cl_2(NMe_2)_4$, 63301-81-5; Mo, 7439-98-7; W, 7440-33-7.

Supplementary Material Available: Tables of anisotropic thermal parameters and complete bond distances and angles (2 pages); listing of F_o and F_c (6 pages). Ordering information is given on any current masthead page.

(21) Buhro, W. E.; Gladysz, J. A. *Inorg. Chem.* **1985**, *24*, 3505.
(22) Cowley, A. H. *Acc. Chem. Res.* **1984**, *17*, 386.
(23) Akiyama, M.; Chisholm, M. H.; Cotton, F. A.; Extine, M. W.; Murillo, C. A. *Inorg. Chem.* **1977**, *16*, 2407.
(24) Tzschach, A.; Deylig, W. *Z. Anorg. Allg. Chem.* **1965**, *336*, 36.
(25) Chisholm, M. H.; Folting, K.; Huffman, J. C. Kirkpatrick, C. C. *Inorg. Chem.* **1984**, *23*, 1021.